Honcharuk Valentyna, Ananevych Iryna, Barchuk Romaniia, Popadynets Oksana. Morpho-Functional Changes in the Skin, Palatal and Buccal Mucosa, and Major Salivary Glands in Iodine Deficiency and Goitrogen Consumption. Journal of Education, Health and Sport. 2024;75:61066. eISSN 2391-8306. https://dx.doi.org/10.12775/JEHS.2024.75.61066
https://apcz.umk.pl/JEHS/article/view/61066
https://zenodo.org/records//15426449

The journal has had 40 points in Minister of Science and Higher Education of Poland parametric evaluation. Annex to the announcement of the Minister of Education and Science of 05.01.2024 No. 32318. Has a Journal's Unique Identifier: 201159. Scientific disciplines assigned: Physical culture sciences (Field of medical and health sciences); Health Sciences (Field of medical and health sciences). Punkty Ministerialne 40 punktów. Załącznik do komunikatu Ministra Nauki i Szkolnictwa Wyższego z dnia 05.01.2024 Lp. 32318. Posiada Unikatowy Identyfikator Czasopisma: 201159. Przypisane dyscypliny naukowe: Nauki o kulturze fizycznej (Dziedzina nauk medycznych i nauk o zdrowiu); Nauki o zdrowiu (Dziedzina nauk medycznych i nauk o zdrowiu).© The Authors 2024;
This article is published with open access at Licensee Open Journal Systems of Nicolaus Copernicus University in Torun, Poland

The authors declare that there is no conflict of interests regarding the publication of this paper.
Received: 21.10.2024. Revised: 17.11.2024. Accepted: 21.11.2024. Published: 23.12.2024.

Morpho-Functional Changes in the Skin, Palatal and Buccal Mucosa, and Major Salivary Glands in Iodine Deficiency and Goitrogen Consumption

Valentyna Honcharuk, Iryna Ananevych, Romaniia Barchuk, Oksana Popadynets

Ivano-Frankivsk National Medical University, Ivano-Frankivsk, Ukraine

Information about authors

Valentyna Honcharuk - Associate Professor, Department of Dermatology and Venereology, Ivano-Frankivsk National Medical University, Ivano-Frankivsk, Ukraine
https://orcid.org/0000-0002-1461-8130
Iryna Ananevych - Assistant Professor, Department of Human Anatomy, Ivano-Frankivsk National Medical University, Ivano-Frankivsk, Ukraine
https://orcid.org/0000-0003-2127-4177
Romaniia Barchuk - Assistant Professor, Department of Human Anatomy, Ivano-Frankivsk National Medical University, Ivano-Frankivsk, Ukraine
https://orcid.org/0000-0002-2680-7895
Oksana Popadynets - DMedSc, Professor, Department of Human Anatomy, Ivano-Frankivsk National Medical University, Ivano-Frankivsk, Ukraine
https://orcid.org/0000-0002-2093-5984

Abstract

Iodine deficiency, combined with daily consumption of natural goitrogens, disrupts thyroid hormone synthesis, resulting in structural and metabolic disturbances within the body. The target organs include the skin, the oral mucosa, and the major salivary glands. Disruptions in these organs provoke changes in multiple systems of the body. However, scientific evidence on the sequential development of morpho-functional changes in these organs under iodine deficiency, in combination with goitrogen consumption, and considering age-related factors,

remains limited. Therefore, the **purpose** of this study was to investigate the morpho-functional changes in the skin, the oral mucosa, and the major salivary glands on the 60th day of iodine deficiency and during goitrogen consumption, considering age-related factors. The experiment was conducted on 50 white non-pedigree male rats, including 25 sexually immature animals (3-5 months old) and 25 sexually mature animals (6-8 months old). Eleven animals from each age group constituted the control group (Group 1). In contrast, 14 animals from each age group were allocated to the experimental groups (Group 2 and Group 3) and exposed to iodine deficiency and goitrogen consumption. Tissue samples were collected on the 60th day of the experiment. Morphological (light microscopy and ultrastructural), morphometric, and biochemical studies were conducted using statistical data processing. In iodine deficiency, accompanied by thyroid status alterations, changes were observed in the epithelium and connective tissue components of the studied organs. Dystrophic-edematous processes progressed in iodine deficiency when combined with the consumption of goitrogens, which exacerbate the hypofunction of the thyroid gland.

Keywords: skin; cheek; palate; parotid salivary gland; submandibular salivary gland; sublingual salivary gland; iodine deficiency; goitrogens

Introduction

The prolonged asymptomatic course of iodine deficiency contributes to its long-term adverse effects on the body [6, 7, 11]. Studies have shown that patients with moderate to severe clinical manifestations of dermatosis exhibit dysfunction of the hypothalamic-pituitary-thyroid axis, which is associated with residence in iodine-deficient regions [2, 3, 10]. The major salivary glands serve as iodine-storing organs, and their function is influenced by the metabolic processes in the body, which are, in turn, regulated by the levels of iodine-containing thyroid hormones [4, 15, 18]. The oral mucosa, through its protective, trophic, excretory, and secretory functions, contributes to the maintenance of homeostasis and serves as a target for various regulatory influences, including hormonal factors [18]. Iodine deficiency, when combined with the consumption of natural goitrogens, such as soy and peanuts, that inhibit thyroid peroxidase, disrupts the synthesis of thyroid hormones and consequently contributes to structural and metabolic imbalances in the body [7, 11, 16]. This condition frequently occurs due to the combined effects of endemic iodine deficiency and specific dietary habits. Nevertheless, this issue remains insufficiently explored in the scientific literature and is addressed only fragmentarily.

The purpose of the study was to investigate morpho-functional changes in the skin, the oral mucosa, and the major salivary glands on the 60th day of iodine deficiency and during goitrogen consumption, considering age-related factors.

Material and Methods

Skin samples were collected from the previously depilated interscapular region of the back and the ventral surface of the limbs (metatarsal pads), the buccal and palatal mucosa, and the parotid, submandibular, and sublingual salivary glands, in addition to blood and urine samples. Iodine deficiency was induced according to the established protocol [9]. Iodine deficiency, combined with the consumption of goitrogens, such as soy and peanuts, was induced according to our patented method [12]. All procedures were carried out with strict adherence to the principles of Humane Animal Treatment. The experiment was conducted on 50 white non-pedigree male rats, including 25 sexually immature animals (3-5 months old) and 25 sexually mature animals (6-8 months old). Eleven animals from each age group constituted the control group (Group 1). In contrast, 14 animals from each age group were allocated to the experimental groups (Group 2 and Group 3) and exposed to iodine deficiency and goitrogen consumption. Tissue samples were collected on the 60th day of the experiment. Morphological (light microscopy and ultrastructural), morphometric, and biochemical studies were conducted using statistical data processing [1].

Results and Discussion

In Group I, the thyroid status in sexually immature animals was as follows: thyroid stimulating hormone (TSH) – 0.10 ± 0.01 μIU/mL ($p < 0.01$), triiodothyronine (T3) – 3.64 ± 0.13 nmol/L ($p < 0.01$), and thyroxine (T4) – 74.59 ± 2.51 nmol/L ($p < 0.01$); in sexually mature animals – 0.08 ± 0.00 μIU/mL ($p < 0.01$), 2.17 ± 0.13 nmol/L ($p < 0.001$), and 55.90 ± 2.67 nmol/L ($p < 0.01$), respectively. Age-specific cholesterol levels were 1.61 ± 0.07 mmol/L ($p < 0.01$) in sexually immature rats and 1.36 ± 0.05 mmol/L ($p < 0.01$) in sexually mature rats. Urinary iodine concentration was 96.69 ± 4.74 μg/L in sexually immature animals and 99.07 ± 4.93 μg/L in sexually mature animals ($p < 0.01$).

In Group II, the thyroid status in sexually immature animals was as follows: TSH – 0.17 ± 0.01 μIU/mL ($p < 0.01$), T3 – 3.56 ± 0.26 nmol/L ($p < 0.001$), and T4 – 76.74 ± 5.84 nmol/L ($p < 0.01$); in sexually mature animals – 0.12 ± 0.01 μIU/mL ($p < 0.01$), 2.98 ± 0.26 nmol/L ($p < 0.01$), and 67.39 ± 4.67 nmol/L ($p < 0.01$), respectively. On day 60 of the experiment, cholesterol levels were 1.66 ± 0.17 mmol/L in sexually immature rats ($p < 0.01$) and 1.40 ± 0.12 mmol/L in sexually mature rats ($p < 0.01$). Urinary iodine concentration was 2.71 ± 0.20 μg/L in sexually immature animals and 3.80 ± 0.37 μg/L ($p < 0.01$) in sexually mature animals.

In Group 2 animals, both sexually immature and mature, light microscopy of skin biopsies from the dorsal and metatarsal pad regions revealed disrupted epidermal architecture, flattened dermal papillae, and focal rarefaction of the dermis, particularly in the perivascular regions (Fig. 1).

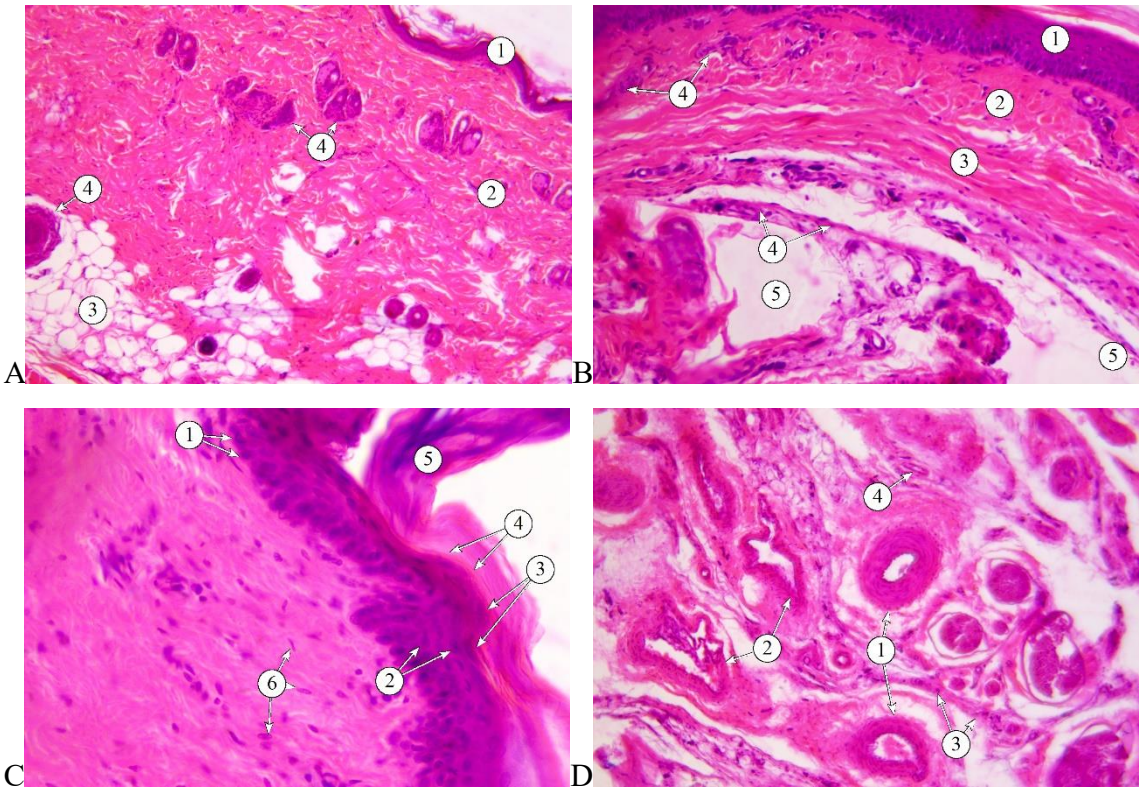

Figure 1. Skin histology in animals with experimentally induced iodine deficiency. A. Dorsal skin of a sexually immature animal: 1 – epidermis, 2 – dermis, 3 – hypodermis, 4 – pilosebaceous units. B. Dorsal skin of a sexually mature animal: 1 – epidermis, 2 – papillary dermis, 3 – reticular dermis, 4 – arteriole, 5 – ground substance. C. Metatarsal pad skin of sexually immature animals: 1 – stratum basale, 2 – stratum spinosum, 3 – stratum granulosum, 4 – stratum lucidum, 5 – stratum corneum, 6 – dermal fibroblasts. D. Metatarsal pad skin of sexually mature animals: 1 – artery, 2 – vein, 3 – arteriole, 4 – hemocapillaries. Hematoxylin and eosin staining. Magnification: A, B – ×100; C – ×200; D – ×400.

In sexually immature animals, the epidermal thickness of the dorsal skin was 17.41 ± 2.77 µm, which represented a 2.4% reduction compared to age-matched controls ($p < 0.001$). In sexually mature animals, the reduction was 0.4% ($p < 0.001$), with a thickness of 19.13 ± 2.80 µm. In contrast, the dermis showed a thickening of 4.9% ($p < 0.001$) in immature animals (527.45 ±

158.84 μm) and 2.7% ($p < 0.001$) in mature animals (580.97 ± 88.93 μm). In sexually immature animals, both the epidermis and dermis of the metatarsal pads showed a slight thickening, by 1.2% ($p < 0.001$) and 1.7% ($p < 0.05$), respectively, with mean thickness values of 134.51 ± 4.08 μm and 725.02 ± 70.34 μm. In sexually mature animals, the epidermis was 1.1% thinner ($p < 0.001$), and the dermis was thinned by 2.3% ($p < 0.01$) compared to age-matched controls, measuring 176.97 ± 4.97 μm and 624.05 ± 143.51 μm, respectively. The hemocapillary lumen diameter in the dorsal skin of sexually immature animals was 7.06 ± 0.64 μm, with a wall thickness of 1.10 ± 0.04 μm. Compared to age-matched controls, the hemocapillary lumen diameter decreased by 1.5% ($p < 0.001$), while the wall thickness increased by 1.9% ($p < 0.001$). These parameters in the dorsal skin of sexually mature animals were 6.39 ± 1.15 μm and 1.05 ± 0.16 μm, respectively, showing a 0.5% ($p < 0.001$) and 3.9% ($p < 0.001$) difference compared to age-matched controls, following the same trend. In the paw skin of sexually immature animals, the hemocapillary lumen diameter decreased by 0.8% ($p < 0.001$), while the wall thickness increased by 1.8% ($p < 0.001$) compared to age-matched controls, measuring 7.14 ± 0.84 μm and 1.13 ± 0.10 μm, respectively. In the paw skin of sexually mature animals, the hemocapillary lumen diameter decreased, and the wall thickness increased by 1.8% ($p < 0.001$), with the respective measurements being 6.50 ± 0.90 μm and 1.11 ± 0.09 μm.

In the buccal and palatal mucosa, the epithelial layers were present; however, cell nuclei were not clearly visualized in all regions. Focal areas representing rarefaction were observed in the lamina propria. Electron microscopy revealed dilated membranous organelles, and hemocapillary endothelial cells exhibited numerous luminal protrusions (Fig. 2, 3).

In Group 2, according to morphometric data, the thickness of the buccal mucosal epithelium in sexually immature animals was 276.63 ± 35.48 μm, which was 1.7% ($p < 0.001$) less than in age-matched controls. In sexually mature animals, it measured 295.71 ± 64.13 μm, which was 4.4% ($p < 0.001$) less than in age-matched controls. The thickness of the lamina propria was 142.76 ± 25.99 μm and 153.19 ± 14.38 μm, respectively, exceeding the control values by 6.3% ($p < 0.001$) and 3.6% ($p < 0.001$), respectively. The hemocapillary lumen diameter in the buccal mucosa of sexually immature animals decreased by 0.4% ($p < 0.001$) compared to age-matched controls, measuring 6.91 ± 1.41 μm, while the wall thickness increased by 0.8% ($p < 0.001$), measuring 1.23 ± 0.29 μm. In sexually mature animals, the hemovascular parameters in the buccal mucosa were 6.29 ± 1.31 μm (0.3% less than in age-matched controls, $p < 0.001$) and 0.97 ± 0.20 μm (1.0% greater than in age-matched controls, $p < 0.001$), respectively.

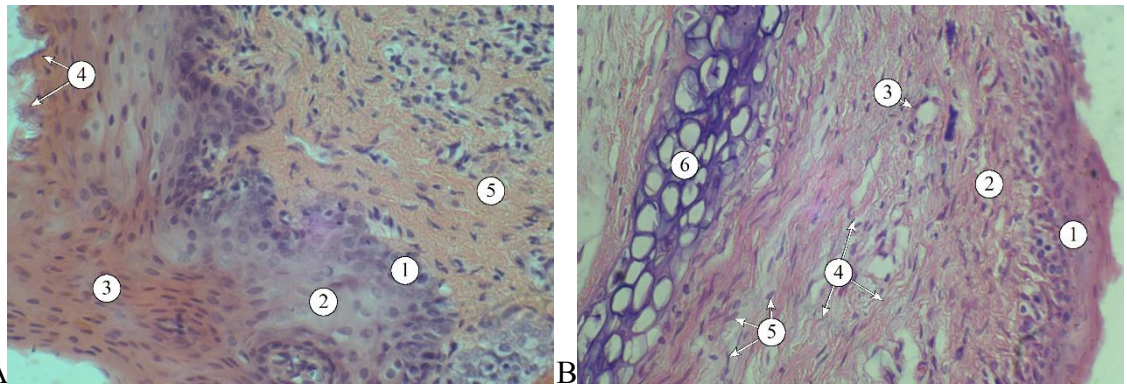

Figure 2. Oral mucosal histology in animals with experimentally induced iodine deficiency. A. Buccal mucosa of a sexually mature animal: 1 – basal cells, 2 – parabasal cells, 3 – intermediate cells, 4 – superficial cells, 5 – lamina propria. B. Palatal mucosa of a sexually immature animal: 1 – epithelium, 2 – lamina propria, 3 – blood vessels, 4 – collagen fibers, 5 – fibroblasts, 6 – adipocytes. Hematoxylin and eosin staining. Magnification: A ×200, B ×100.

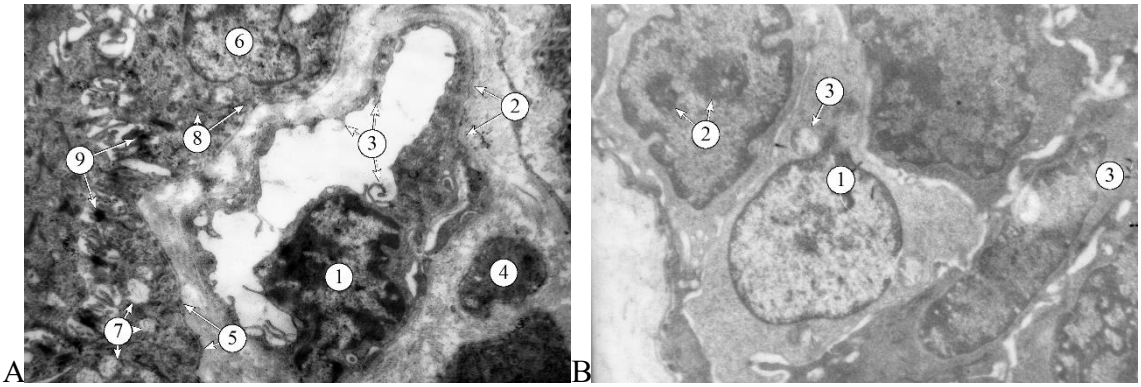

Figure 3. Oral mucosal ultrastructure in animals with experimentally induced iodine deficiency. A. Buccal mucosa of a sexually immature animal: 1 – endothelial cell nucleus, 2 – hemocapillary basement membrane, 3 – luminal protrusions of endothelial cell, 4 – pericyte nucleus, 5 – basement membrane, 6 – epithelial cell nucleus, 7 – mitochondria, 8 – rough endoplasmic reticulum, 9 – desmosomes. B. Palatal mucosa of a sexually mature animal: 1 – epithelial cell nucleus, 2 – nucleolus, 3 – mitochondria. Electron micrographs. Magnification: A, B ×6,400.

The thickness of the palatal mucosal epithelium in Group 2 sexually immature animals was 95.49 ± 10.42 μm, and in sexually mature animals, it was 93.65 ± 15.84 μm, which was 2.7% ($p < 0.001$) and 16.7% ($p < 0.001$) less than in age-matched controls, respectively. The thickness

of the lamina propria was 128.18 ± 14.42 µm and 134.17 ± 22.19 µm, respectively, exceeding the control values by 5.7% ($p < 0.001$) and 4.2% ($p < 0.001$), respectively. The hemocapillary lumen diameter and wall thickness in the palatal mucosa of sexually immature animals were 6.87 ± 0.96 µm and 1.11 ± 0.09 µm, respectively. Compared to the age-matched control, the lumen diameter decreased by 0.4% ($p < 0.001$), while the wall thickness increased by 1.8% ($p < 0.001$). In sexually mature animals, the corresponding parameters were 6.09 ± 0.67 µm and 0.95 ± 0.06 µm, respectively, showing a similar trend, with changes of 0.5% ($p < 0.001$) and 1.1% ($p < 0.001$), respectively.

Light microscopy of the parotid, submandibular, and sublingual salivary glands revealed identifiable secretory units and duct systems. The connective tissue components were clearly separated, and the stroma exhibited areas of rarefaction (Fig. 4).

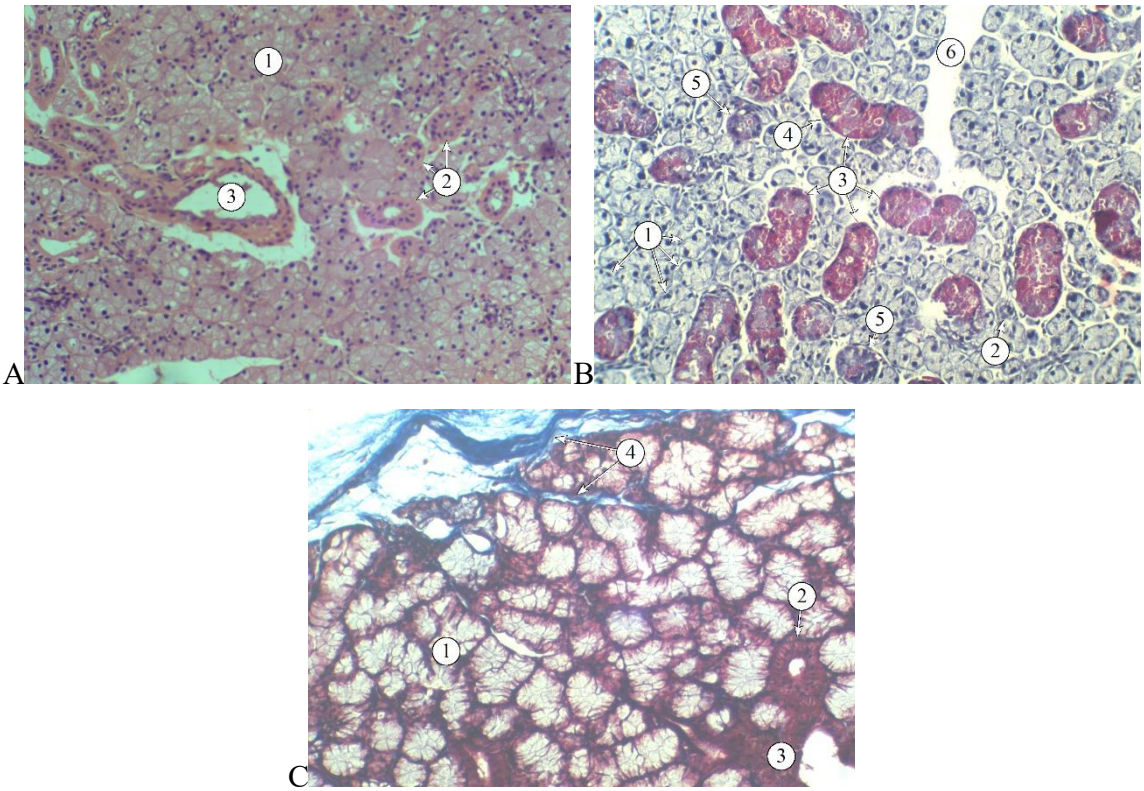

Figure 4. Histology of the major salivary glands in animals with experimentally induced iodine deficiency. A. Parotid salivary gland of a sexually immature animal: 1 – secretory units, 2 – striated ducts, 3 – interlobular ducts. B. Submandibular salivary gland of a sexually immature animal: 1 – secretory units, 2 – intercalated duct, 3 – granular duct, 4 – myoepithelial cell of the granular duct, 5 – striated duct, 6 – interlobular septa. C. Sublingual salivary gland of a sexually mature animal: 1 – secretory units, 2 – striated duct, 3 – interlobular duct, 4 – collagen fibers. Staining: A – hematoxylin and eosin, B, C – Masson's trichrome. Magnification: ×200.

In electron microscopy, the epithelial cells of the secretory units and ducts displayed dilated organelles of the synthetic apparatus and vacuolated mitochondria with disorganized cristae (Fig. 5).

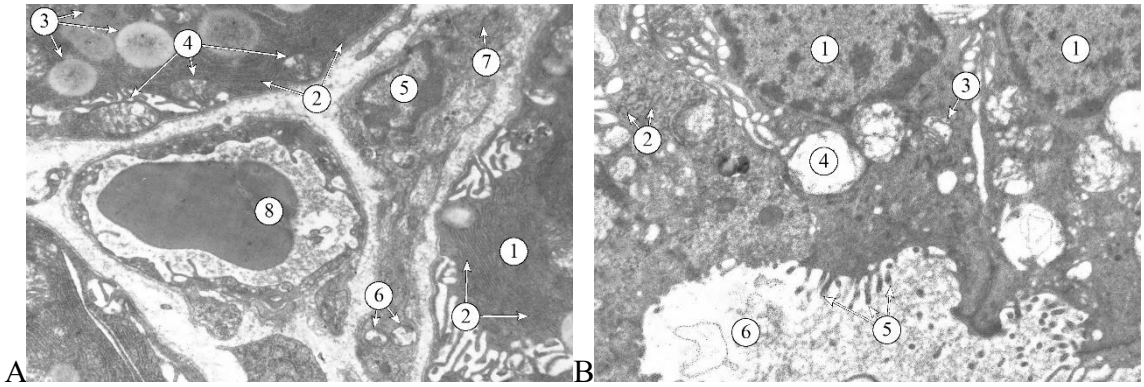

Figure 5. Ultrastructure of the major salivary glands in animals with experimentally induced iodine deficiency. A. Parotid salivary gland of a sexually mature animal: 1 – epithelial cell cytoplasm, 2 – rough endoplasmic reticulum, 3 – secretory granules, 4 – mitochondria, 5 – fibroblast nucleus, 6 – fibroblast mitochondria, 7 – Golgi apparatus in the fibroblast cytoplasm, 8 – erythrocyte in the hemocapillary lumen. B. Sublingual salivary gland of a sexually immature animal: 1 – epithelial cell nucleus, 2 – rough endoplasmic reticulum, 3 – mitochondria, 4 – secretory granules, 5 – apical microvilli, 6 – duct lumen. Electron micrographs. Magnification: ×8,000.

In Group 2 sexually immature animals, according to morphometric data, the surface area of serous cells in the parotid salivary gland was 126.88 ± 20.19 μm², while in sexually mature animals, it was 115.58 ± 13.04 μm², which was 1.7% ($p < 0.001$) and 4.7% ($p < 0.001$) greater than in age-matched controls, respectively. The relative optical density of the secretory granules was 0.15 ± 0.03 and 0.20 ± 0.03, respectively, with the values in sexually mature animals being 4.8% ($p < 0.001$) lower than in age-matched controls. The hemocapillary lumen diameter in the parotid salivary gland of sexually immature animals was 6.36 ± 0.76 μm, which was 3.2% ($p < 0.001$) smaller than in age-matched controls, while the wall thickness was 1.24 ± 0.23 μm, representing a 1.6% ($p < 0.001$) increase compared to the age norm. In sexually mature animals, the corresponding parameters were 5.98 ± 0.48 μm (2.3% ($p < 0.001$) less than the age norm) and 1.04 ± 0.11 μm, which was 0.9% ($p < 0.001$) greater than the control value, respectively.
The surface area of seromucous cells in the submandibular salivary gland of sexually immature and mature animals was 134.84 ± 24.31 μm² and 126.53 ± 12.63 μm², respectively, which

exceeded the age-matched control values by 2.6% ($p < 0.001$) and 2.9% ($p < 0.001$). The relative optical density of the secretory granules in sexually immature and mature animals was 0.11 ± 0.01 and 0.14 ± 0.03, respectively; in sexually immature animals, it was 8.3% ($p < 0.001$) lower compared to age-matched controls. In the submandibular salivary gland of sexually immature animals, the hemocapillary lumen diameter and wall thickness were 6.61 ± 1.16 μm and 1.27 ± 0.11 μm, respectively, which were 1.8% ($p < 0.001$) lower and 1.6% ($p < 0.001$) higher than the age-matched norm. In sexually mature animals, these parameters were 6.13 ± 1.12 μm and 1.02 ± 0.19 μm, showing a 0.5% ($p < 0.001$) decrease and a 0.9% ($p < 0.001$) increase, respectively, compared to age-matched controls.

In Group 2 sexually immature and mature animals, the surface area of mucocytes in the sublingual salivary gland was 164.92 ± 29.82 μm² and 154.11 ± 14.78 μm², respectively, which was 0.8% ($p < 0.001$) and 1.7% ($p < 0.001$) greater than in age-matched controls. The relative optical density of the secretory granules was 0.09 ± 0.01 and 0.10 ± 0.01, corresponding to 18.2% ($p < 0.001$) and 16.7% ($p < 0.001$) of the age norm, respectively. In the sublingual salivary gland of sexually immature animals, the hemocapillary lumen diameter and wall thickness were 6.72 ± 1.16 μm (3.4% [$p < 0.001$] less than in age-matched controls) and 1.29 ± 0.13 μm (1.6% [$p < 0.001$] more than in age-matched controls), respectively. In sexually mature animals, the corresponding parameters were 6.01 ± 0.80 μm (2.9% [$p < 0.001$] less than in age-matched controls) and 1.05 ± 0.12 μm (0.9% [$p < 0.001$] more than in age-matched controls), respectively

In Group 3, the thyroid status of sexually immature animals was as follows: TSH – 0.18 ± 0.02 μIU/mL ($p < 0.01$), T3 – 3.46 ± 0.25 nmol/L ($p < 0.01$), and T4 – 76.12 ± 7.47 nmol/L ($p < 0.01$); in sexually mature animals – 0.14 ± 0.01 μIU/mL ($p < 0.01$), 2.38 ± 0.21 nmol/L ($p < 0.01$), and 70.06 ± 4.66 nmol/L ($p < 0.01$), respectively. Cholesterol level on day 60 of the experiment was 1.62 ± 0.12 mmol/L ($p < 0.01$) in sexually immature rats and 1.44 ± 0.12 mmol/L ($p < 0.01$) in sexually mature rats. Urinary iodine concentration was 1.40 ± 0.11 μg/L ($p < 0.01$) in sexually immature animals and 1.88 ± 0.13 μg/L ($p < 0.01$) in sexually mature animals.

Histological examination of the paw and dorsal skin in Group 3 animals, both sexually immature and mature, revealed poorly defined stratification of the epidermis, flattened dermal papillae, and rarefaction in the papillary and reticular layers of the dermis (Fig. 6).

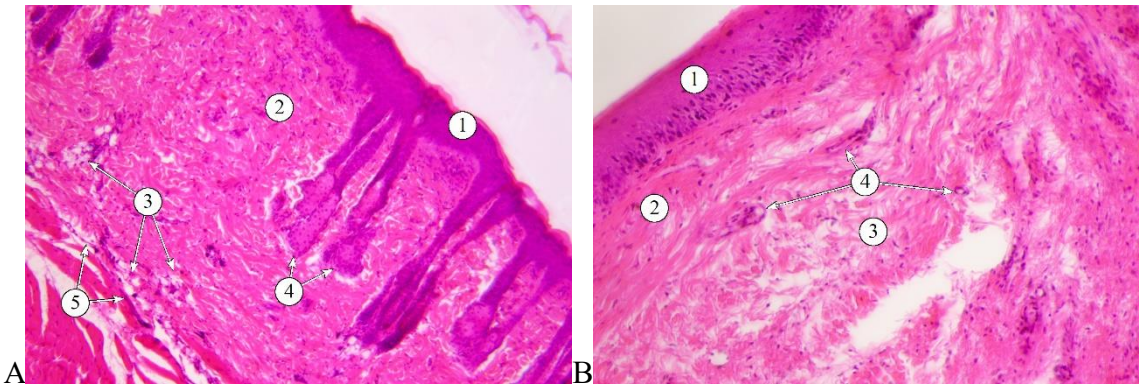

Figure 6. Skin histology in animals with experimentally induced iodine deficiency and goitrogen consumption. A. Dorsal skin of a sexually immature animal: 1 – epidermis, 2 – dermis, 3 – hypodermis, 4 – sebaceous glands, 5 – blood vessels. B. Metatarsal pad skin of a sexually mature animal: 1 – epidermis, 2 – papillary dermis, 3 – reticular dermis, 4 – blood vessels. Hematoxylin and eosin staining. Magnification: A ×100, B ×200.

The morphometric parameters were found to be changed. In the dorsal skin of sexually immature animals, the epidermal thickness was 17.28 ± 1.98 µm ($p < 0.001$), and the dermal thickness was 556.87 ± 123.86 µm ($p < 0.01$). In sexually mature animals, these parameters were 19.01 ± 1.97 µm ($p < 0.001$) and 600.42 ± 90.18 µm ($p < 0.001$), respectively. The hemocapillary lumen diameter in the dorsal skin of sexually immature animals was 7.02 ± 1.33 µm ($p < 0.001$), while the wall thickness was 1.12 ± 0.09 µm ($p < 0.001$).

In the dorsal skin of sexually mature animals, the corresponding parameters were 6.28 ± 0.91 µm ($p < 0.001$) and 1.11 ± 0.16 µm ($p < 0.01$), respectively. In the skin of the metatarsal pads of sexually immature animals, the epidermal and dermal thicknesses were 135.60 ± 14.03 µm ($p < 0.001$) and 746.55 ± 114.17 µm ($p < 0.001$), respectively. In sexually mature animals, the epidermal thickness was 181.03 ± 6.33 µm ($p < 0.001$), while the dermal thickness was 641.46 ± 126.20 µm ($p < 0.001$). In the skin of the metatarsal pads of sexually immature animals, the hemocapillary lumen diameter and wall thickness were 7.09 ± 1.23 µm ($p < 0.001$) and 1.16 ± 0.03 µm ($p < 0.001$), respectively. In sexually mature animals, these parameters were 6.47 ± 1.08 µm ($p < 0.001$) and 1.13 ± 0.22 µm ($p < 0.001$), respectively.

Dystrophic changes in the epithelium, edema in the lamina propria, diffuse clusters of glycosaminoglycans, and hemostasis were observed in the buccal and palatal mucosa (Fig. 7).

Electron microscopy confirmed the findings of light microscopy. In epithelial cells, organelles appeared dilated, and mitochondria exhibited a lucent matrix. Signs of stasis were observed in

blood vessels. Collagen fibers were surrounded by a ground substance of low electron density. Organelles of the synthetic apparatus were clearly identifiable in fibroblasts (Fig. 8).

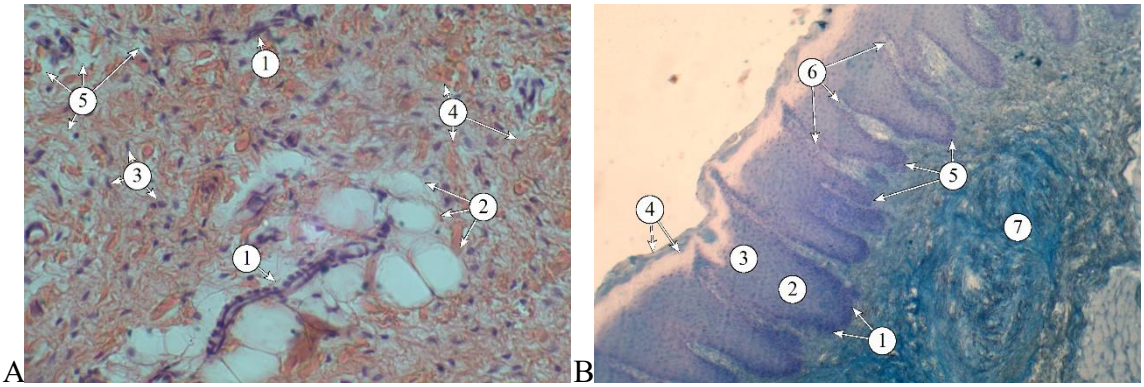

Figure 7. Oral mucosal histology in animals with experimentally induced iodine deficiency and goitrogen consumption. A. Buccal mucosa of a sexually immature animal: 1 – arteriole, 2 – adipocytes, 3 – fibroblasts, 4 – connective tissue fibers, 5 – ground substance. B. Palatal mucosa of a sexually mature animal: 1 – basal cells, 2 – stratum spinosum epithelial cells, 3 – stratum granulosum epithelial cells, 4 – keratinized cells, 5 – epithelial ridges, 6 – connective tissue papillae, 7 – glycosaminoglycan deposits in the lamina propria. Staining: A – hematoxylin and eosin; B – Stidman's method. Magnification: ×200.

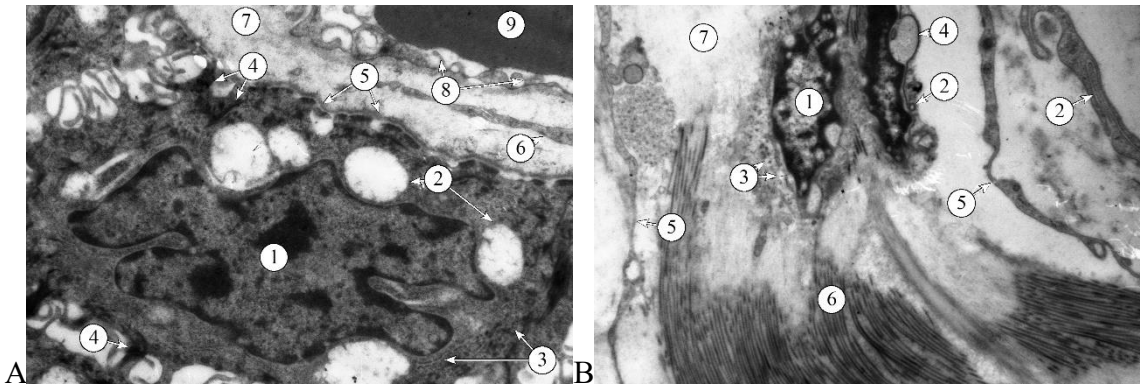

Figure 8. Oral mucosal ultrastructure in animals with experimentally induced iodine deficiency and goitrogen consumption. A. Buccal mucosa of a sexually mature animal: 1 – epithelial cell nucleus, 2 – mitochondria, 3 – rough endoplasmic reticulum, 4 – desmosomes, 5 – basement membrane, 6 – fibroblast process, 7 – ground substance, 8 – luminal protrusions of endothelial cell, 9 – erythrocyte. B. Palatal mucosa of a sexually immature animal: 1 – fibroblast nucleus, 2 – rough endoplasmic reticulum, 3 – Golgi apparatus, 4 – mitochondria, 5 – fibroblast process, 6 – collagen fibers, 7 – ground substance. Electron micrographs. Magnification: A ×8,000, B ×6,400.

In Group 3, the epithelial thickness of the buccal mucosa in sexually immature animals was 258.27 ± 41.14 μm, and in sexually mature animals, it was 268.15 ± 53.09 μm, being 8.2% ($p < 0.001$) and 13.3% ($p < 0.001$) lower, respectively, compared to age-matched controls. The thickness of the lamina propria within the buccal mucosa in sexually immature and mature animals was 161.48 ± 31.09 μm and 168.41 ± 39.81 μm, respectively, exceeding age-matched controls by 20.3% ($p < 0.001$) and 13.9% ($p < 0.001$), respectively. The hemocapillary lumen diameter in the buccal mucosa of sexually immature animals measured 6.90 ± 1.01 μm ($p < 0.001$), with a wall thickness of 1.24 ± 0.11 μm ($p < 0.001$). In sexually mature animals, the corresponding hemovascular parameters were 6.26 ± 0.73 μm ($p < 0.001$) and 0.98 ± 0.10 μm ($p < 0.001$), respectively.

The epithelial thickness of the palatal mucosa in Group 3 sexually immature and mature animals was 94.08 ± 18.20 μm and 83.81 ± 10.74 μm, respectively, which was 4.1% ($p < 0.001$) and 25.5% ($p < 0.001$) lower than the age-matched control data. At this stage of the experiment, the thickness of the lamina propria within the palatal mucosa was 130.78 ± 20.41 μm and 139.79 ± 20.49 μm in sexually immature and mature animals, respectively, exceeding age-matched controls by 7.9% ($p < 0.001$) and 8.5% ($p < 0.001$), respectively. The hemocapillary lumen diameter in the palatal mucosa of sexually immature animals measured 6.86 ± 0.98 μm ($p < 0.001$), with a wall thickness of 1.12 ± 0.10 μm ($p < 0.001$). In sexually mature animals, the hemocapillary lumen diameter and wall thickness were 6.07 ± 0.80 μm ($p < 0.001$) and 0.96 ± 0.07 μm ($p < 0.001$), respectively

Edema was observed in the epithelial cells of the secretory regions, the ductal system, and the stromal components of the major salivary glands (Fig. 9).

Electron microscopy revealed noticeable organelle growth, the presence of blood formed elements within the lumen of blood vessels, and perivascular edema (Fig. 10).

In Group 3, the surface area of serous cells in the parotid salivary gland was 129.67 ± 11.99 μm² ($p < 0.001$) in sexually mature animals and 118.49 ± 9.84 μm² ($p < 0.001$) in sexually immature animals. The relative optical density of the secretory granules was 0.15 ± 0.01 ($p < 0.001$) in sexually mature animals and 0.20 ± 0.02 ($p < 0.001$) in sexually immature animals. The hemocapillary lumen diameter in the parotid salivary gland of sexually immature animals measured 6.24 ± 1.24 μm ($p < 0.001$), with a wall thickness of 1.25 ± 0.12 μm ($p < 0.001$). In sexually mature animals, the corresponding parameters were 5.71 ± 1.08 μm ($p < 0.001$) and 1.04 ± 0.19 μm ($p < 0.001$), respectively.

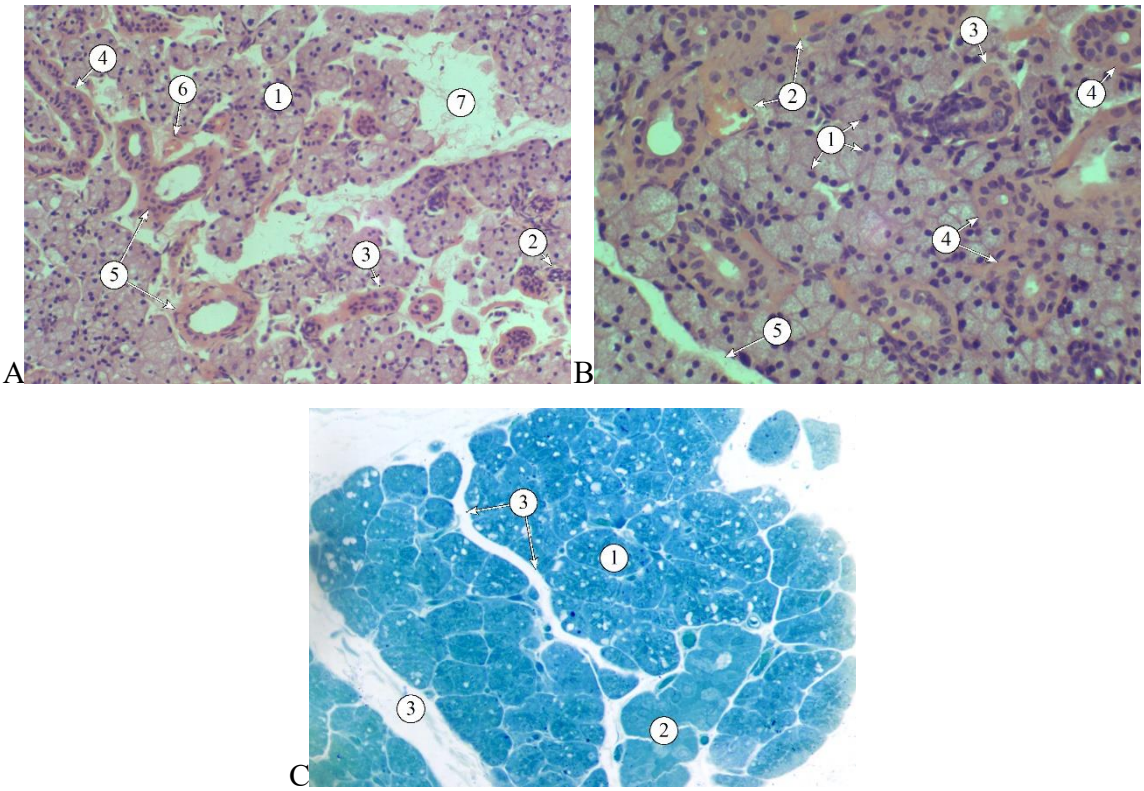

Figure 9. Histology of the major salivary glands in animals with experimentally induced iodine deficiency and goitrogen consumption. A. Parotid salivary gland of a sexually mature animal: 1 – secretory units, 2 – intercalated ducts, 3 – small striated ducts, 4 – large striated ducts, 5 – interlobular ducts, 6 – blood vessels, 7 – connective tissue fibers and ground substance. B. Submandibular salivary gland of a sexually mature animal: 1 – seromucous cell nuclei, 2 – blood vessels, 3 – granular duct, 4 – striated duct, 5 – connective tissue layers. C. Sublingual salivary gland of a sexually immature animal, semithin section: 1 – secretory units, 2 – interlobular excretory duct, 3 – connective tissue layers. Staining: A, B – hematoxylin and eosin; C – methylene blue. Magnification: A, C ×100, B ×200.

The surface area of seromucous cells in the submandibular salivary gland was 135.48 ± 11.51 μm² ($p < 0.001$) and 128.09 ± 20.00 μm² ($p < 0.001$), respectively. The relative optical density of the secretory granules was 0.10 ± 0.01 ($p < 0.001$) and 0.13 ± 0.02 ($p < 0.001$), respectively. In the submandibular salivary gland of sexually immature animals, the hemocapillary lumen diameter and wall thickness were 6.59 ± 1.04 μm ($p < 0.001$) and 1.28 ± 0.21 μm ($p < 0.001$), respectively. In sexually mature animals, the corresponding parameters were 6.11 ± 0.96 μm ($p < 0.001$) and 1.02 ± 0.09 μm ($p < 0.001$), respectively.

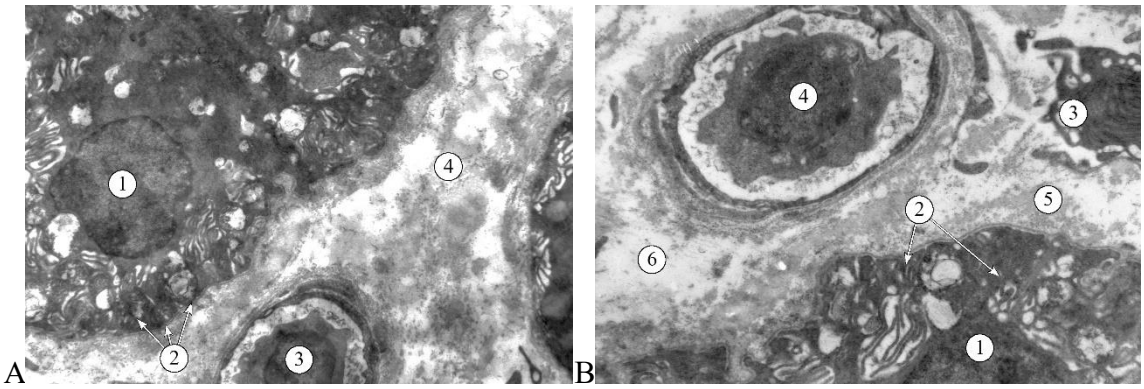

Figure 10. Ultrastructure of the major salivary glands in animals with experimentally induced iodine deficiency and goitrogen consumption. A. Submandibular salivary gland of a sexually immature animal: 1 – epithelial cell nucleus in the striated duct, 2 – mitochondria in the invaginations of the basal plasma membrane, 3 – lymphocyte in the hemocapillary lumen, 4 – ground substance. B. Sublingual salivary gland of a sexually mature animal: 1 – epithelial cell nucleus, 2 – basal striation, 3 – fibroblast, 4 – monocyte in the hemocapillary lumen, 5 – collagen fibers, 6 – ground substance. Electron micrographs. Magnification: ×6,400.

The surface area of mucocytes in the sublingual salivary gland was 167.12 ± 13.64 μm² ($p < 0.001$) and 156.04 ± 24.71 μm² ($p < 0.001$), respectively. The relative optical density of the secretory granules in animals of both age groups was 0.09 ± 0.01 ($p < 0.001$). In the sublingual salivary gland of sexually immature animals, the hemocapillary lumen diameter and wall thickness were 6.63 ± 1.61 μm ($p < 0.001$) and 1.31 ± 0.13 μm ($p < 0.001$), respectively. In sexually mature animals, these parameters were 5.78 ± 0.56 μm ($p < 0.001$) and 1.06 ± 0.21 μm ($p < 0.001$), respectively.

Thus, morpho-functional changes were observed in all the studied organs, with their severity progressing in iodine deficiency combined with goitrogen consumption. The epidermal and dermal indicators from various regions suggest the influence of thyroid imbalance, as the skin contains three isoforms of thyroid hormone receptors [8, 14, 17]. These receptors directly affect proteoglycan synthesis in the skin by stimulating fibroblasts [6, 14]. The reduction in catabolic processes leads to the accumulation of hyaluronic acid in the dermis [2, 6]. Salivary glands accumulate iodine due to the presence of the sodium-iodide symporter, which transports iodine from the blood to the saliva [18]. Iodine deficiency disrupts the lipid profile [5, 13] and is accompanied by impaired blood circulation. The observed reduction in the hemocapillary lumen, accompanied by thickening of the vessel walls and the presence of edematous perivascular connective tissue components, confirms the disruption of trophic support.

Consequently, the secretory function of the major salivary glands and the mucous membranes of both the lining and masticatory types (cheeks and palate) is impaired [15].

Conclusions

At the stages of sexual maturation, the skin, the oral mucosa, and the major salivary glands are primary targets for thyroid hormone action. Iodine deficiency leads to structural and metabolic disturbances within the body, resulting in dystrophic-edematous changes in the epithelial layer and connective tissue components. The reduction in the hemocapillary lumen, coupled with thickening of the hemocapillary walls, disrupts trophic processes and impairs the secretory function of the epithelium. Morpho-functional changes are more pronounced in iodine deficiency combined with goitrogen consumption.

Perspectives for further research involve tracking the structural and metabolic changes in the skin, the buccal and palatal oral mucosa, and the major salivary glands as iodine deficiency progresses and goitrogens are consumed.

References

1. Bahrii MM, Dibrova VA, Popadynets OH, Hryshchuk MI. Methods of morphological research: a monograph. Bahrii MM, Dibrova VA, editors. Vinnytsia: Nova Knyha; c2016. 328p. Ukrainian.

2. Costa GM, Araujo SL, Félix Xavier Júnior FA, de Araújo Viana D, Evangelista JSAM. Dermatological manifestations associated with canine hypothyroidism: a review. A Revista Brasileira de Higiene e Sanidade Animal. 2016;10(4):781-97. Available from: https://doi.org/10.5935/1981-2965.20160064

3. Gade A, Hwang JR, Hoegler K, Khan S, Khachemoune A. Therapeutic use of trace elements in dermatology. Altern Ther Health Med. 2023;29(4):246-52.

4. Guo W, Pan Z, Zhang Y, Jin Y, Dong S, Wu W, et al. Saliva iodine concentration in children and its association with iodine status and thyroid function. J Clin Endocrinol Metab. 2020;105(9):e3451–9. Available from: https://doi.org/10.1210/clinem/dgaa471

5. Jung KY, Ahn HY, Han SK, Park YJ, Cho BY, Moon MK. Association between thyroid function and lipid profiles, apolipoproteins, and high-density lipoprotein function. J Clin Lipidol. 2017;11(6):1347-53. Available from: https://doi.org/10.1016/j.jacl.2017.08.015

6. Karvatska YuP. Indicators of the pituitary-thyroid and immune systems in patients with acne from iodine-deficient regions, depending on the severity of dermatosis. Ukrainian Scientific and Practical Conference with International Participation “Your Dermatological Rebus”. 2019 April 4-5. Dnipro, Ukraine. Available from: http://repo.dma.dp.ua/id/eprint/5589. Ukrainian.

7. Kukharchuk KhM. Clinical and epidemiological features of cardiovascular pathology in young people with subclinical hypothyroidism. Health of Society. 2019;8(3):106-11. Ukrainian.

8. Mancino G, Sibilio A, Luongo C, Di Cicco E, Miro C, Cicatiello AG, et al. The thyroid hormone inactivator enzyme, type 3 deiodinase, is essential for coordination of keratinocyte growth and differentiation. Thyroid. 2020;30(7):1066-78. Available from: https://doi.org/10.1089/thy.2019.0557

9. Martínez-Galán JR, Pedraza P, Santacana M, Escobar del Ray F, Morreale de Escobar G, Ruiz-Marcos A. Early effects of iodine deficiency on radial glial cells of the hippocampus of the rat fetus. A model of neurological cretinism. J Clin Invest. 1997;99(11):2701-9. Available from: https://doi.org/10.1172/JCI119459

10. Niaz F, Shams N, Meraj L, Ahmed S, Ahmed N, Sheikh I. Skin changes in newly diagnosed cases of hypothyroidism. JRMC. 2022;26(1):83-9. Available from: https://doi.org/10.37939/jrmc.v26i1.1762

11. Pankiv VI, Yuzvenko TYu. Relationships of subclinical thyroid dysfunction and metabolic syndrome. Clin Endocrinol Endocr Surg (Ukraine). 2017;2(58):39-43. Available from: https://doi.org/10.24026/1818-1384.2(58).2017.105577 Ukrainian

12. Popadynets OH, Sahan OV, Barchuk RR, Voianskyi RS, Ananevych IM, Sahan NT, et al. Method for modeling iodine-deficient conditions with the addition of goitrogenic products. Patent of Ukraine No. 111647, 2016. Ukrainian.

13. Ranhulova T. Non-alcoholic fatty liver disease and hypothyroidism: review of clinical and experimental studies. Galician Medical Journal. 2021;28(4):E202142. Available from: https://doi.org/10.21802/gmj.2021.4.2

14. Ruiz-Llorente L, Contreras-Jurado C, Martínez-Fernández M, Paramio JM, Aranda A. Thyroid hormone receptors regulate the expression of microRNAs with key roles in skin homeostasis. Thyroid. 2018;28(7):921-32. Available from: https://doi.org/10.1089/thy.2017.0369

15. Saraswathi G, Harini BK. Oral manifestations of metabolic disorders - a comprehensive review. IJRR. 2024;11(5):302-6. Available from: https://doi.org/10.52403/ijrr.20240535

16. Skrypnyk NV. Metabolic syndrome and hypothyroidism: pathogenetic interrelations, diagnosis, and treatment. Diabetology, Thyroidology, Metabolic Disorders. 2017;1(37):60-3. Ukrainian.

17. Srujana B, Narayan Reddy B, Prasad GK. Clinical spectrum of cutaneous manifestations of thyroid disorders in patients attending MediCiti Institute of Medical Sciences. IP Indian J Clin

Exp Dermatol. 2016;2(4):146-52. Available from: https://doi.org/10.18231/2455-6769.2016.0006

18. Yeroshenko GA, Shevchenko KV, Kramarenko DR, Vilkhova OV, Yachmin AI. Dysfunction of the salivary glands – actual medical and social problem. Bulletin of problems biology and medicine. 2019;1(150):22-6. Available from: https://doi.org/10.29254/2077-4214-2019-2-1-150-22-26 Ukrainian.